The fine structure of Pearlman's catalyst

Peter W. Albers, Konrad Möbus, Stefan D. Wieland and Stewart F. Parker

Published version information

Citation: Albers, PW et al. "The fine structure of Pearlman's catalyst." Physical Chemistry Chemical Physics, vol. 17, no. 7 (2015): 5274-5278.

doi: 10.1039/C4CP05681G

PCCP

RSCPublishing

ARTICLE

The Fine Structure of Pearlman's Catalyst

Cite this: DOI: 10.1039/xoxxoooooox

Peter W. Albers,[a*] Konrad Möbus,[b] Stefan D. Wieland,[b] and Stewart F. Parker[c]

Received ooth January 2012,
Accepted ooth January 2012

DOI: 10.1039/xoxxoooooox

www.rsc.org/

Pearlman's catalyst, nominally $Pd(OH)_2/C$, is widely used as for hydrogenation reactions and C-C coupling reactions. Contrary to the accepted view, we show that Pearlman's catalyst as prepared and after drying consists of carbon supported (mostly) nano-particulate hydrous palladium oxide capped with a monolayer of hydroxyls hydrogen-bonded to a few layers of water: a core-shell structure of $C/PdO/OH/H_2O$. The conventional formulation $Pd(OH)_2/C$ from the macroscopic point of view is ruled-out by the different spectral signatures of surface hydroxyls and stoichiometric hydroxides. We also show that a minor fraction of the palladium is present as a reduced species.

Introduction

Pearlman's catalyst[1,2], is used in various hydrogenation and hydrogenolysis reactions[3,4], it is also effective in various C-C coupling reactions (*e.g.*) Fukuyama, Sonogashira and Suzuki coupling[5-7]. It is also used as an O-debenzylation agent. A prominent practical feature is that in spite of the high precious metal loading this versatile material is non-pyrophoric.

The catalyst is commonly written as palladium (II) hydroxide supported on carbon, $Pd(OH)_2/C$. However, we have recently shown[8] that a typical commercial sample of unsupported hydrous palladium oxide consists of a poorly crystalline core of PdO ~1.8 nm in diameter capped with a monolayer of hydroxyls and all covered with several layers of water. Thus it is a core-shell structure rather than uniform stoichiometric $Pd(OH)_2$. This may dominate the topmost surface layers which previously were investigated by X-ray photoelectron spectroscopy.[9] In view of this result, there must be a strong suspicion that the commonly accepted formulation of Pearlman's catalyst is an approximation from the macroscopic point of view and its fine structure still needs to be investigated in more detail. Knowledge of the state of the palladium is important in trying to understand the mechanism of the reactions since recent work has suggested that the catalyst functions by leaching of palladium into solution.[10] It was concluded 'that a homogeneous catalyst species is generated under the reaction conditions and that this species is responsible for the observed catalysis' and that palladium hydroxide on carbon 'is a convenient source of a phosphine-free homogeneous catalyst'.[10] Leaching into the solution has also been observed for Pd/C catalysts.[11,12] Clearly the dissolution (and re-deposition onto the carbon support as a heterogenisation of a homogeneous catalyst) of $Pd(OH)_2$ will be different from that of PdO and of metallic Pd. This has been previously observed in mobility studies of commercial palladium black and PdO at different pH values and varying access of organic molecules.[13] Furthermore, the pH-dependence of the water/palladium/hydroxyl ratio in polynuclear hydroxo-palladium complexes and the influence of temperature and ageing on cluster sizes have to be taken into account.[14]

The use of high surface area carbons as the support and enhanced precious metal loading (typically 5 - 20 wt.%) in the Pearlman's catalyst means that conventional vibrational spectroscopy is inapplicable (because of absorption of light (Infrared and Raman)) or fluorescence (Raman) in studying the detailed structure. Inelastic incoherent neutron scattering (IINS) spectroscopy was essential to reveal the properties of hydrous palladium oxide and is also the technique of choice here. IINS can readily distinguish between hydroxides and water. The presence of carbon can complicate the IINS analysis somewhat, however, the availability of large (25 g) sample quantities and of the pure carbon support enabled us to obtain definitive spectra of the "palladium (II) hydroxide" on the catalyst.

Experimental Section

Catalysts

5 wt.% and 20 wt.% Pearlman's catalyst (Evonik Industries) were measured in the original water-wet state (w) and after drying *in-vacuo* (d) Table 1. The activated carbon support was measured as a reference. Details on the preparation of this grade of catalyst are outlined in Refs.[1, 15].

Hydrogen content

The hydrogen content of the activated carbon catalyst support was determined by hot extraction using a LECO TCH600 instrument.

Transmission Electron Microscopy (TEM)

A Jeol 2010F field emission transmission electron microscope was operated at 200 keV acceleration voltage. A catalyst sample was dispersed in chloroform and transferred onto holey carbon foil supported by a 200 mesh copper grid. For statistical evaluation of the primary particle sizes of the supported primary particles the I-TEM software of Soft Imaging Systems (SIS), Münster, Germany, was utilized. The average primary particle sizes of the supported Pd-based catalyst particles were determined by statistical evaluation of 2000 particles in TEM images per catalyst sample. The quality, stability and calibration of the TEM system were maintained by the use of the Magical No. 641 standard (Norrox Scientific Ltd., Beaver Pond, Ontario, Canada).

X-ray Photoelectron Spectroscopy (XPS)

A Thermo Fisher 250 Xi instrument electron energy analyzer was operated at 72 eV in the fixed analyzer transmission mode. A catalyst sample was introduced as a loose powder. Integral XPS spectra of an area of 650 µm spot diameter were recorded using monochromatised AlK_{α} radiation.

Inelastic Incoherent Neutron Scattering (IINS)

Each catalyst and the unloaded support sample for background subtraction was sealed into a thin-walled (0.5 mm) stainless steel (1.4571) can which was closed by a top-flange with a stainless steel pipe and a welded bellows valve (Nupro) via OFHC-copper (oxygen-free high conductivity) gasket (pressure and safety test certificate: RLI 533). A sealed can containing macroscopic amounts of catalyst (precise values in Table 1) was evacuated using a turbo-molecular pump which was backed by a dual stage rotary pump with a zeolite trap to avoid back-diffusion of oil and other potential molecular contaminants. IINS spectra were recorded using the spectrometers MAPS[16] and TOSCA[17,18] at the spallation neutron source ISIS. [-19] On TOSCA the resolution is ~1.25% of the energy transfer across the entire energy range, while on MAPS, under the conditions used here, it is ~1.5% of the incident energy at the largest energy transfer and degrades with decreasing energy transfer. Thus TOSCA provides excellent energy resolution at energy transfers < 1200 cm^{-1}, at larger energy transfer MAPS provides better resolution by virtue of the access to low momentum transfer.[16] TOSCA and MAPS are highly complementary and enable the complete range of interest, 0 – 4000 cm^{-1}, to be covered with good resolution. A sample can was quenched down into liquid nitrogen, loaded in a closed cycle helium cryostat and measured at 20 K.

Table 1 IINS sample specification

Sample No.	composition	IINS sample weight (g)	humidity (wt.%)
1	5% Pd/C w	59.48	58.80
2	5% Pd/C d	20.63	[a]
3	20% Pd/C w	51.50	55.30
4	20% Pd/C d	27.95	[a]
5	activated carbon support [b]	18.60	[a]

[a] Dried at 105°C for 12 h in a vacuum chamber. [b] Hydrogen content of support 0.49 % +/- 0.04% H.

Results and Discussion

Morphology and size of the supported particles

The morphology and distribution of the palladium entities in the 5% and the 20% catalysts are similar (Figure 1 and Table 2). The average primary particles size and its standard deviation in the 20% sample is only slightly enhanced compared to the 5% catalyst. Narrow particle size distributions were obtained in both cases (only small differences between DN and DA). Lattice imaging of the precious metal particles (Figure 2) revealed d-spacings of mostly 0.26 nm which is indicative for both, palladium oxide and hydrous oxide.[20] Additionally, but only to a minor extend, 0.19 and 0.23 nm lattice spacings were observed indicative of metallic palladium.[20]

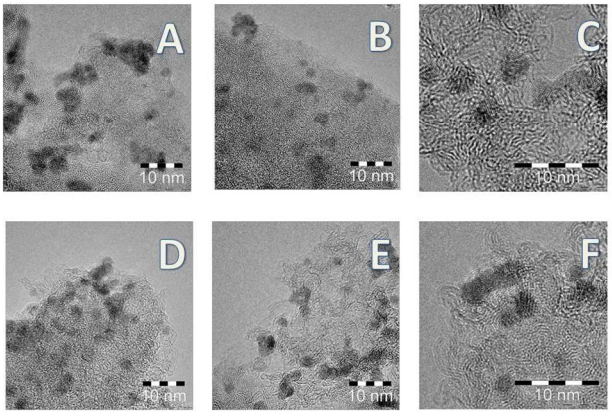

Fig. 1 TEM micrographs of the dried Pearlman's catalysts; A-C: 5% D-F: 20% precious metal loading.

Table 2 Results of particle size evaluation from TEM micrographs

Pd content	DN[a]	S_{DN}[b]	DA[c]	EMS[d]
(wt.%)	(nm)	(nm)	(nm)	(m^2g^{-1})
5	2.34	0.25	2.39	208.1
20	2.40	0.29	2.50	202.3

[a] DN and [b] S_{DN} : primary particle size (arithmetical average) and its standard deviation; DN=($\Sigma n_i d_i$)/N; [c] DA: primary particle size averaged over the surface, DA=($\Sigma n_i d_i^3$) /($\Sigma n_i d_i^2$); [d] EMS: calculated electron microscopic surface; EMS= 6000/(DA x ρ); ρ_{Pd} : 11.99 g cm^{-3}.

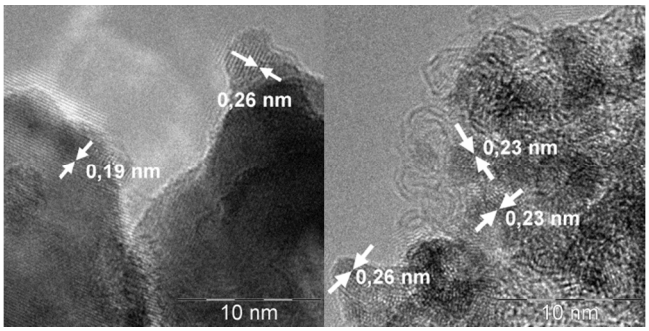

Fig. 2 TEM lattice imaging; reference values for the d-spacing in Ref. [20] .

Surface chemistry

These observations are confirmed by means of XPS of the topmost surface region (Figure 3, Table 3). The palladium 3d signal region contains at least two doublets (Figure 3, right). Gaussian/Lorentzian line shape analyses reveal the presence of ca. 13-17% of a species at ca. 335.3-335.7 eV and about 87-83% of at ca. 336-337 eV. The Pd-species in the ca. 335-336 eV binding energy region can be assigned to the small amounts of crystallites of reduced palladium (Figure 2, d-values 0.19 nm and 0.23 nm) with slight surface oxidation/hydroxylation and the Pd-species in the region ca. 336-337 eV to bivalent palladium oxide and palladium hydroxides together with residual water molecules in hydrogen bonding[9, 21, 22] the latter being the target for the neutron scattering experiments due to the high sensitivity to hydrogen of IINS.

Figure 3 and Table 3 illustrate that for the topmost atomic layers the drying procedure caused minor (5% Pd catalyst) and larger (20% Pd catalyst) changes of the surface composition (Pd/O/C) and of the O/Pd-ratio, whereas only small differences in the ratios of different valency states of the precious metal occur.

Comparing the carbon values of the 5% and 20% catalyst it appears that the good dispersion of the palladium/oxygen entities leads to a pronounced shielding of the carbon support by the well dispersed palladium species and by water molecules (Figure 1). Removal of the weaker adsorbed water molecules leads to a more pronounced uncovering of the palladium and of the carbon support on the 20% Pd catalyst. The XPS signals in the oxygen 1s region (plus $Pd3p_{3/2}$) at ca. 529-530 eV can be assigned to lattice oxygen of the PdO and the contributions at ca. 533-535 eV (including the asymmetric signal broadening) to hydroxides and adsorbed water. In a previous study an O1s binding energy of 534.1 eV was observed for supported ice.[23]

The results suggest the presence of about 13-17% of reduced supported Pd-species in addition to the dominating amount of mainly bivalent precious metal oxide particles. Due to the partial Pd/O-signal overlap (Figure 3, left), more detailed information on the surface hydroxyl- and oxy-hydrate groups needs to be obtained from IINS due to the high penetrating power of the neutron compared to the surface selectivity of XPS.

Table 3 XPS-results; surface concentrations (at.%) and results of Gaussian/ Lorentzian line shape approximations.

Catalyst	1: 5% w	2: 5% d	3: 20% w	4: 20% d
Pd 3d (%)[a]	1.9	2.0	9.2	13.3
O1s (%)[b]	11.7	10.7	35.3	25.5
C1s (%)[c]	86.4	87.3	56.5	61.2
$Pd3d_{5/2}$ (%) ca. 335-336 eV	14.6	16.6	16.5	12.9
$Pd3d_{5/2}$ (%) ca. 336-337 eV	85.4	83.4	83.5	87.1

Relative sensitivity factors: [a] $Pd3d_{5/2}$ 9.48, $Pd3d_{3/2}$ 6.56; [b] O1s 2.93; [c] C1s 1.00. For the determination of the surface oxygen concentration the partial overlap of the $Pd3p_{3/2}$ signal with the O1s region was taken into account. Reference values in [9, 21, 22] .

Inelastic incoherent neutron scattering: core-shell structure

Comparing the IINS spectrum of the wet Pd(5%)/C catalyst to that of ice I_h [24] in Figure 4 it can be seen that the spectra are almost identical, thus the water present completely dominates the spectrum. Only minor differences in the shape and position of the steep leading edge of the librational mode region of the water (ca. 540 cm^{-1}) and the translational modes (< ca. 300 cm^{-1}) are apparent between the supported (a) ice and the bulk (b) of ice I_h occur. This undoubtedly arises because of the large water (>50 wt%, Table 1) of the as received catalysts

Figure 5 shows the IINS spectra of the dried catalysts and the bare carbon support. The difference spectra: ([20 wt% Pd/C] – C) and ([5 wt% Pd/C] – C) are shown in Figure 6. The difference spectra show a broad band centred at ~500 cm^{-1} and a feature at 960 cm^{-1} that is poorly defined for the 5 wt% Pd/C sample but sharp for the 20 wt% Pd/C sample. Comparison with the spectrum of hydrous palladium oxide dried at 100 °C [8], Figure 6, shows a striking

similarity and the spectra are assigned accordingly: the broad feature is the librational modes of a disordered water layer and the 960 cm^{-1} feature is the Pd–O–H bending mode of surface hydroxyls. The assignment to surface hydroxyls is supported by periodic-DFT calculations of hydroxyls on PdO[8] and that the bending mode of hydroxyls on alumina[25] and silica[26] occur in this region where water does not have any modes.

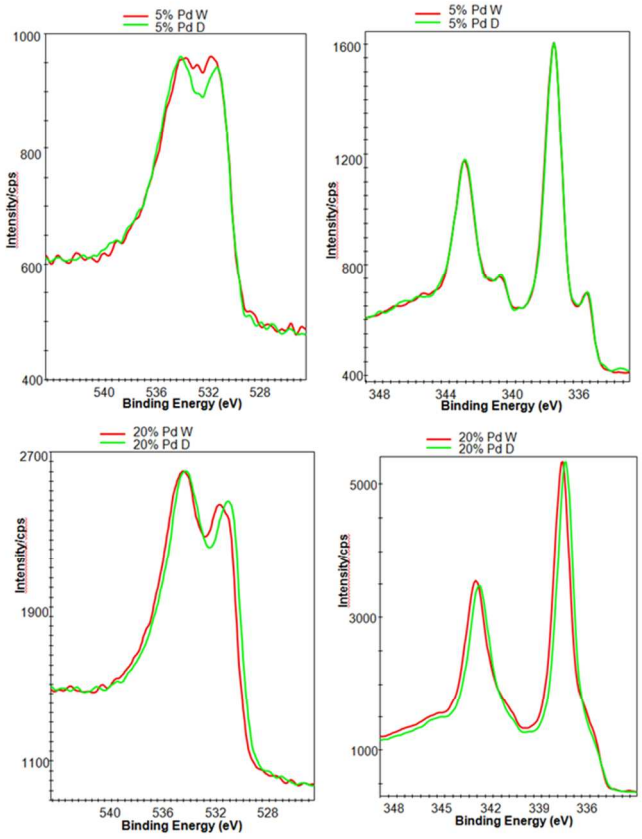

Fig. 3 XPS signals of the catalysts 1-4. Left: oxygen 1s signal region; right: palladium $3d_{5/2}$ and $3d_{3/2}$ doublet region; upper: 5%, lower: 20% catalyst.

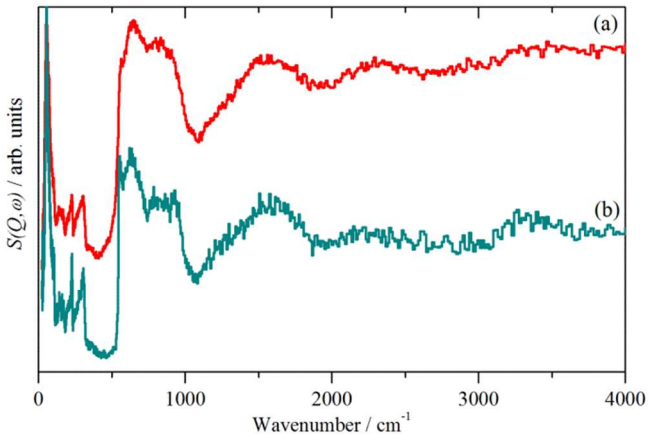

Fig. 4 Comparison of the (TOSCA) IINS spectrum of: (a) the wet Pd(5%)/C sample and (b) ice I_h both recorded at 20K.

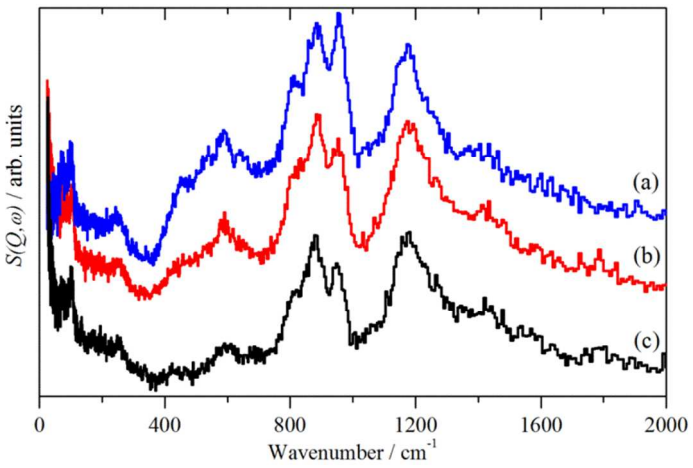

Fig. 5 Comparison of the (TOSCA) IINS spectra of the dried catalysts (a) 20 wt% Pd/C, (b) 5 wt% Pd/C and (c) the carbon support.

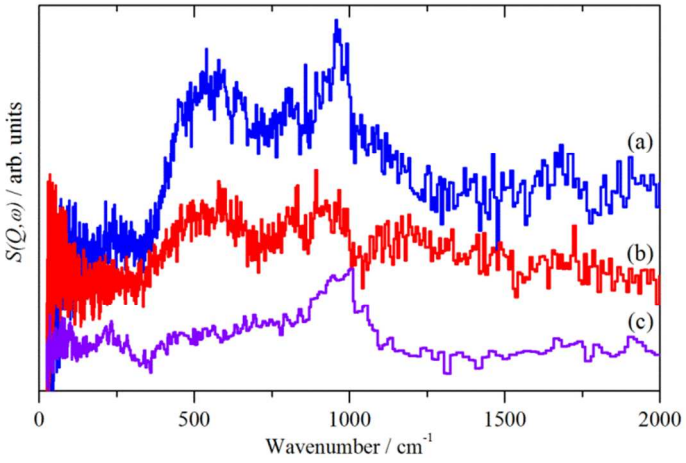

Fig. 6 Comparison of the difference spectra of the dried samples: (a) ([20 wt% Pd/C] – C), (b) ([5 wt% Pd/C] – C) with that of (c) hydrous palladium oxide dried at 100 °C.[8]

The assignment of the broad feature to water is confirmed in Figures 7 and 8 that show the IINS spectra of the dried Pd(20%)/C sample and the carbon support recorded on MAPS in the C–H/O–H stretch region and the deformation region. In the high energy region, Figure 7, the difference spectrum clearly shows features at 1570 and 3470 cm^{-1} that are unambiguously assigned to the H-O-H scissors mode and the O–H stretch of water respectively[27] . The presence of water is likely due to insufficient drying and there is residual water on the activated carbon support. Drying pure, unsupported, hydrous palladium oxide at 100 °C does not remove all the adsorbed water[8] In this case, the five to seven layers of water initially present are reduced to one or two layers of water on drying, presumably reflecting the stronger hydrogen bonding between the surface hydroxyls and the adsorbed water than between the disordered water layers.

Comparison of the carbon support and the Pd(20%)/C sample in the deformation region, Figure 8, shows the presence of the sharp Pd–O–H bending mode at ~960 cm^{-1}. There are additional modes associated with the Pd–O–H moiety, however, even on pure hydrous palladium oxide[8] only the bending mode was clearly seen. The hydrogen bonding between the water and the hydroxyls means that the hydroxyl O–H stretch forms part of the broad band at 3470 cm^{-1}. Periodic-DFT calculations[8] confirm that the Pd–O–H bending mode is the only mode that occurs in a region that is not obscured by other modes.

.

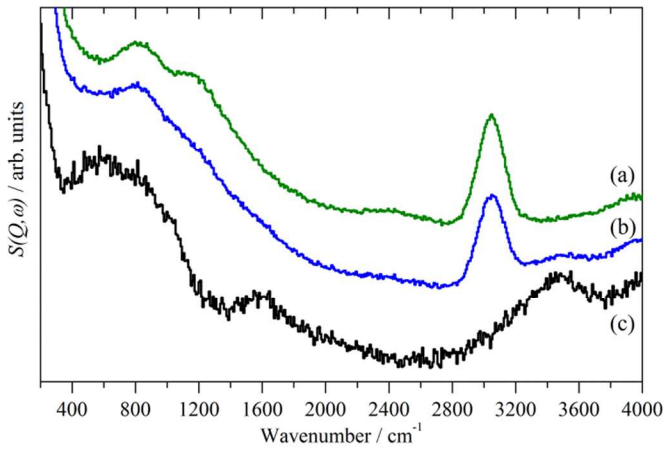

Fig. 7 INS spectra recorded on MAPS of (a) the carbon support, (b) the dried Pd(20%)/C sample and (c) the difference spectrum recorded on MAPS.

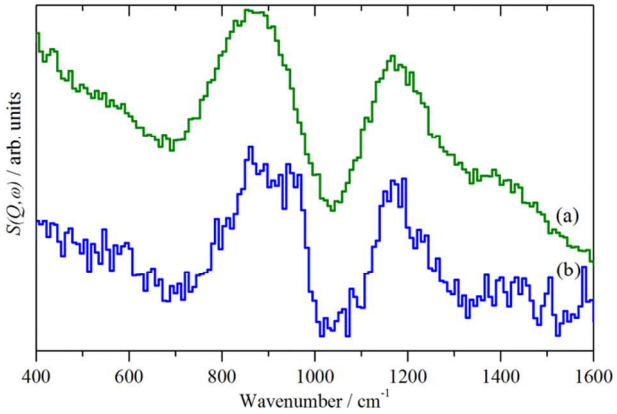

Fig. 8 INS spectra of (a) the carbon support and (b) the dried Pd(20%)/C sample recorded on MAPS in the deformation region.

Conclusions

All of the evidence presented here is consistent with our suggestion that Pearlman's catalyst should be formulated as C/PdO/OH/H_2O *i.e.* hydrous palladium oxide supported on carbon, rather than uniform stoichiometric $Pd(OH)_2$/C, palladium (II) hydroxide supported on carbon. The TEM data show lattice spacings typical of palladium oxide and hydrous oxide in agreement with XPS which shows the major phase contains Pd(II). The IINS data show the presence of water and hydroxyls. These must be surface-OH rather than a stoichiometric hydroxide[28] because the latter have a characteristic, and very different, spectral signature to surface hydroxyls.[8,] The IINS spectra of the supported materials after drying show a remarkable similarity to that of partially dried hydrous palladium oxide, Figure 6. The unexpected result revealed by the TEM and XPS studies is the presence of a minority fraction, ca. 13-17%, of nearly metallic palladium. Since Pearlman's catalyst is generally used in non-aqueous environments[3-7] this species may simply be a spectator species in the C–C coupling reactions that are one of the major uses of Pearlman's catalyst. This supports work[6] that showed that Pd/C is a much less effective catalyst for Fukuyama, Sonogashira and Suzuki coupling reactions than Pearlman's catalyst. The reduced palladium could be formed by a reducing influence of the carbonaceous support during catalyst preparation.

Acknowledgements

The STFC Rutherford Appleton Laboratory is thanked for access to neutron beam facilities.

Notes and references

[a*]AQura GmbH, D-63457 Hanau/Wolfgang, Germany. E-Mail: peter.albers@aqura.de; Tel.: +49 6181 59 2934
[b] Evonik Industries AG, Inorganic Materials, Business Line Catalysts, D-63457 Hanau/Wolfang, Germany.
[c] ISIS Facility, STFC Rutherford Appleton Laboratory, Chilton, Didcot, OX11 0QX, United Kingdom.

References

1 W.M. Pearlman, *Tetrahedron Lett.*, 1967, **8**, 1663-1664.

2 Pearlman's catalyst: *Comprehensive Organic Name Reactions and Reagents,* 2010, 2143-2146.

3 S.R. Angle, R.M. Henry, *J. Org. Chem.*, 1997, **62**, 8549-8552.

4 L. Yin, J. Liebscher, *Chem. Rev.,* 2007, **107**, 133-173.

5 Y. Mori, M. Seki, *Heterocycles,* 2002, **58**, 125-127.

6 Y. Mori, M. Seki, *J. Org. Chem.*, 2003, **68,** 1571-1574.

7 M. Kimura, M. Seki, *Tetrahedron Lett*., 2004, **45**, 1635-1637 .

8 S.F. Parker, K. Refson, A.C. Hannon, E. Barney, S.J. Robertson, P. Albers, *J. Phys. Chem. C,* 2010, **114**, 14164-14172.

9 S.H. Oh, G.B. Hoflund, *J. Catal.,*. 2007, **245**, 35-44.

10 M. Parisien, D. Valette, K. Fagnou, *J. Org. Chem.,* 2005, **70,** 7578-7584.

11 K. Köhler, R. G. Heidenreich, J.G.E. Krauter, J. Pietsch, *Chem. Eur. J.*, 2002, **8**, 622-631.

12 R. G. Heidenreich, K. Köhler, J. G. E. Krauter, *Synlett.*, 2002, **7**, 1118-1122.

13 F. Zereini, C. L. S. Wiseman, M. Vang, P. Albers, W. Schneider, R. Schindl, and K. Leopold, 14. Edelmetall-Forum, Universität Ulm, S. 1-3; J. Popritzki and F. Zereini, 14. Edelmetall-Forum, Universität Ulm; DFG project GZ:ZE950/2-1; F. Zereini, C. L. S. Wiseman, M. Vang, P. Albers, W. Schneider, R. Schindl, K. Leopold, submitted to Environ. Sci. Technol., manuscript es-2014-05222a.

14 V.A. Semikolenov, *Russ. Chem. Rev.,* 1992, **61**, 168-174; translation downloaded from http.://iopscience.iop.org/0036-021X/61/2/R03.

15 Shigeo Nishimura, *Handbook of Heterogeneous Catalytic Hydrogenation for Organic Synthesis*, Wiley, New York, 2001, p. 37.

16 S.F. Parker, D. Lennon, P.W. Albers, *Applied. Spectroscopy*, 2011, **65,** 1325-1341.

17 S.F. Parker, F. Fernandez-Alonso, A.J. Ramirez-Cuesta, J. Tomkinson, S. Rudic, R.S. Pinna, G. Gorini, J. Fernández Castañon, *Journal of Physics Conference Series*, 2014, **554**, 012003.

18 P.C.H. Mitchell, S.F. Parker, A.J. Ramirez-Cuesta, J. Tomkinson, *Vibrational Spectroscopy with Neutrons: with applications in Chemistry, Materials Science and Catalysis*, World Scientific, Singapore, **2005** p. 104-108 and p.524.

19 http://www.isis.stfc.ac.uk/

20 International Centre for diffraction data, JCPDS, Newton Square, Pennsylvania/USA, 1995; Pd (111) 0.22462 nm, (200) 0.1945 nm; PdO (101)0.2644 nm; PdO_2 (211) 0.1681 nm; $PdOxH_2O$ (101) 0.2615 nm, (112) 0.1668 nm.

21 *Practical Surface Analysis 2nd Edition*, *Volume 1*, (Eds.: D. Briggs and M.P. Seah), John Wiley, Chichester, 1990, p.613.; Pd: R. Nyholm, N. Martensson, *Solid State Commun.,* 1981, **40**, 311-314. PdO, PdO_2: K.S. Kim, A.F. Grossmann, N. Winograd, *Anal. Chem.,* 1974**, 46**. 197-200.

22 http://srdata.nist.gov/xps/ElmSpectralSrch.aspx?selEnergy=PE

23 P. Albers, A. Karl, J. Mathias, D.K. Ross, S.F. Parker, *Carbon,* 2001, **39**, 1663-1676.

24 J.-C. Li, *J. Chem. Phys*., 1996, **105**, 6733-6755.

25 D. Lennon, S.F. Parker, *Accounts of Chemical Research* 2014, **47**, 1220-1227.

26 P. Hoffmann, E. Knözinger *Surf. Sci.* 1987, **188**, 181.

27 J.-C. Li, J. D. Londono, D. K. Ross, J. L. Finney, S. M. Bennington, A. D. Taylor, *J. Phys.: Condens. Matter,* 1992, **4**, 2109-2116.

28 R. Baddour-Hadjean, F. Fillaux, N. Floquet, S. Belushkin, I. Natkaniec, L. Desgranges, D. Grebile, *Chem. Phys.,* 1995, **197**, 81-90.

